Cell

Replication-Coupled Chromatin Assembly Generates a Neuronal Bilateral Asymmetry in *C. elegans*

Shunji Nakano,[1,3] Bruce Stillman,[2] and H. Robert Horvitz[1,*]
[1]Howard Hughes Medical Institute and Department of Biology, Massachusetts Institute of Technology, Cambridge, MA 02139, USA
[2]Cold Spring Harbor Laboratory, 1 Bungtown Road, Cold Spring Harbor, NY 11724, USA
[3]Present address: Division of Biological Science, Graduate School of Science, Nagoya University, Nagoya 464-8602, Japan
*Correspondence: horvitz@mit.edu
DOI 10.1016/j.cell.2011.11.053

SUMMARY

Although replication-coupled chromatin assembly is known to be important for the maintenance of patterns of gene expression through sequential cell divisions, the role of replication-coupled chromatin assembly in controlling cell differentiation during animal development remains largely unexplored. Here we report that the CAF-1 protein complex, an evolutionarily conserved histone chaperone that deposits histone H3-H4 proteins onto replicating DNA, is required to generate a bilateral asymmetry in the *C. elegans* nervous system. A mutation in 1 of 24 *C. elegans* histone H3 genes specifically eliminates this aspect of neuronal asymmetry by causing a defect in the formation of a histone H3-H4 tetramer and the consequent inhibition of CAF-1-mediated nucleosome formation. Our results reveal that replication-coupled nucleosome assembly is necessary to generate a bilateral asymmetry in *C. elegans* neuroanatomy and suggest that left-right asymmetric epigenetic regulation can establish bilateral asymmetry in the nervous system.

INTRODUCTION

Anatomical and functional bilateral asymmetries of the brain are widespread features of humans and other animals and are thought to be important for behavior and cognitive functions (Toga and Thompson, 2003). Abnormal brain lateralization has been implicated in several neuropathologies, including autism and schizophrenia (Escalante-Mead et al., 2003; Li et al., 2007). Although the *nodal* signaling pathway has been shown to be central in establishing left-right asymmetry in visceral organs (Levin, 2005; Shiratori and Hamada, 2006), expression of the *nodal* signaling genes has not been detected in the developing mammalian brain (Hamada, 2008). Nonetheless, the mouse hippocampus has been shown to display molecular bilateral asymmetry (Kawakami et al., 2003). Thus, despite its importance, the molecular mechanisms that generate brain bilateral asymmetry remain largely elusive.

Although mostly bilaterally symmetric, the *C. elegans* nervous system displays a variety of bilateral asymmetries (Hobert et al., 2002). For example, the MI motor neuron is a single left-right unpaired neuron located in the pharynx (Albertson and Thomson, 1976). The MI neuron is generated from an invariant left-right asymmetric cell lineage in which the blastomere ABaraap divides and generates two daughter cells, ABaraapa and ABaraapp, that give rise to identical sets of left-right paired cells, except for two cells, the left-right unpaired MI neuron on the right side of the cell lineage and the e3D pharyngeal epithelial cell on the left (Sulston et al., 1983) (Figure 1A). Thus, the generation of the single unpaired MI neuron results from the disruption of the bilateral symmetry in this cell lineage.

We previously showed that the establishment of the MI-e3D asymmetry requires asymmetric expression of a transcriptional cascade in which the *Otx* homeodomain protein CEH-36 is expressed in the MI grandmother cell but not in the e3D grandmother cell and CEH-36 promotes asymmetric expression of two proneural bHLH proteins, NGN-1 and HLH-2, in the MI mother cell but not in the e3D mother cell (Nakano et al., 2010). Inactivation of any component of the CEH-36/NGN-1/HLH-2 cascade transforms the MI neuron into an e3D-like cell, resulting in the loss of the MI-e3D asymmetry. How this transcriptional asymmetry is transduced into the postmitotic MI neuron remained to be determined.

Here we report that chromatin assembly factor-1 (CAF-1), which deposits histone H3-H4 proteins onto replicating DNA (Smith and Stillman, 1989), is required to generate the MI-e3D asymmetry. We find that a mutation in 1 of 24 histone H3 genes can cause the loss of the MI-e3D bilateral asymmetry. This histone H3 mutation causes a defect in the formation of a histone H3-H4 tetramer and the consequent inhibition of CAF-1-mediated nucleosome formation. Our results indicate that replication-coupled de novo nucleosome assembly in the MI mother cell is required to generate a chromatin mark that is then transmitted to the postmitotic MI neuron. We suggest that left-right asymmetric epigenetic regulation is involved in the establishment of the neuronal bilateral asymmetry and that epigenetic regulation similarly acts to generate neuronal bilateral asymmetry in mammals through a mechanism independent of *nodal* signaling.

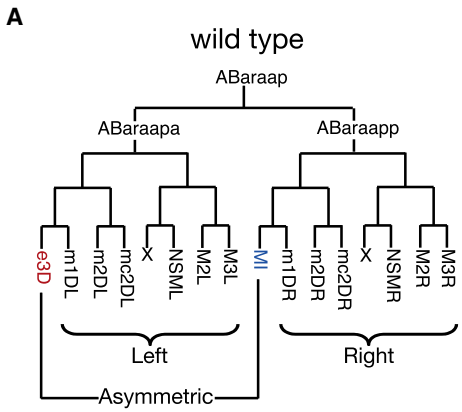

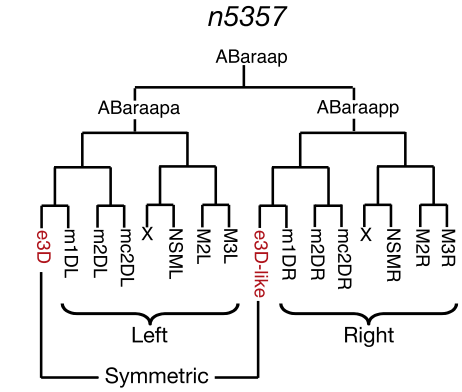

C

Genotype	% MI transformation 25 °C	20 °C	15 °C
wild-type	0 (*n* = 50)	0 (*n* = 50)	0 (*n* = 50)
n5357/n5357	2 (*n* = 81)	24 (*n* = 104)	55 (*n* = 123)
n5357/+	0 (*n* = 102)	2 (*n* = 173)	8 (*n* = 234)

D

n5357 locus	% MI transformation
n5357/n5357	24 (*n* = 82)
n5357/n5357/+	26 (*n* = 85)

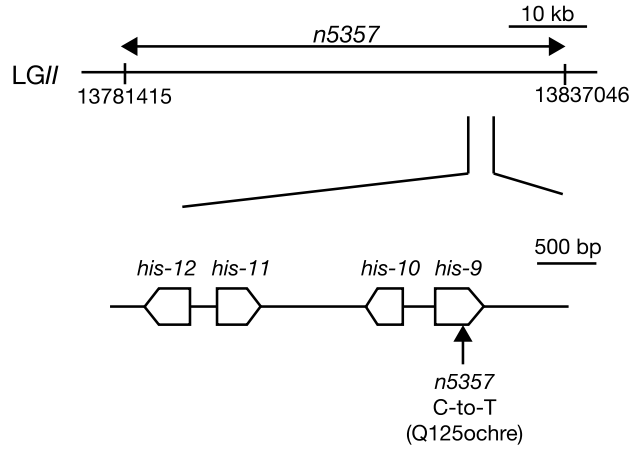

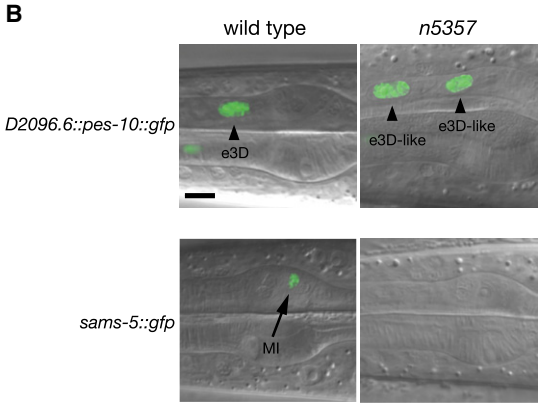

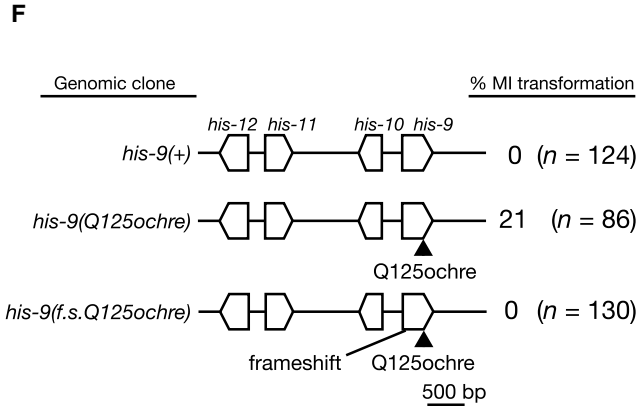

Figure 1. *n5357* Is a Gain-of-Function Allele of a Histone H3 Gene and Causes the Loss of the MI-e3D Bilateral Asymmetry

(A) The ABaraap cell lineages in the wild-type and *n5357* mutants.

(B) Expression of the *D2096.6::pes-10::gfp* and *sams-5::gfp* reporters in a wild-type and an *n5357* animal. The arrowheads indicate e3D and the extra e3D-like cell. The arrow indicates the MI neuron. Scale bar, 5 μm.

(C and D) Percentage of animals showing the MI transformation defect. The MI transformation defects in (D) were determined at 15°C. We noted that the MI transformation defect of *n5357/n5357* animals in (D) was less severe than that of *n5357/n5357* animals in (C) and found that this difference was caused by a background mutation(s) present in the *n5357/n5357* strain used in (D) (see Experimental Procedures).

(E) A physical map of the *n5357* region and the location of a mutation in the *his-9* locus of *n5357* animals are shown. The numbers indicate the chromosome coordinates to which we mapped the *n5357* mutation.

(F) Germline transformation experiments using genomic *his-9* clones. The structure of each genomic clone and the percentage of animals showing the MI transformation defect at 15°C are shown.

See also Figure S1.

RESULTS

A Histone H3 Mutant Eliminates the MI-e3D Bilateral Asymmetry

To elucidate the mechanism that establishes the MI-e3D asymmetry, we performed genetic screens with an e3D cell-fate reporter, *D2096.6::pes-10::gfp* (Nakano et al., 2010), and sought mutants in which an extra e3D-like cell was present or e3D was absent (our unpublished data). Among the isolates we recovered was the mutation *n5357,* which caused the presence of an extra e3D-like cell (Figure 1B). We introduced an MI cell-fate reporter, *sams-5::gfp* (Nakano et al., 2010), into *n5357* mutants and observed that MI was missing in *n5357* animals (Figure 1B), indicating that MI is transformed into an e3D-like cell, thereby resulting in the loss of the MI-e3D bilateral asymmetry (Figure 1A). *n5357* causes a cold-sensitive and semidominant phenotype (Figure 1C). To determine whether *n5357* is a gain- or loss-of-function mutation, we performed a gene-dosage study and found that the presence of a free duplication chromosome covering the *n5357* region neither enhanced nor suppressed the MI transformation defect caused by *n5357* (Figure 1D and Experimental Procedures). This result indicates that *n5357* is a gain-of-function mutation and is likely an altered-function mutation.

We mapped *n5357* to a 55 kb interval of chromosome II that contains a cluster of 13 predicted histone genes (Figure 1E). We performed DNA sequence analysis of *n5357* and identified a mutation in the gene *his-9*, which encodes a histone H3 protein (Pettitt et al., 2002). The sequence of the 135 amino acid HIS-9 protein displays a higher degree of identity to those of the human replication-dependent histones H3.1 and H3.2 than to that of the replication-independent histone H3.3 (Figure S1). The *C. elegans* genome contains 24 histone H3 loci, 14 of which are replication-dependent histone H3 genes that encode proteins with amino acid sequences identical to that of the HIS-9 protein (Pettitt et al., 2002). *n5357* animals carry a transition mutation that is predicted to alter the glutamine 125 codon to an ochre stop codon (Figure 1E). To test whether this DNA lesion is responsible for the MI transformation of *n5357* animals, we generated genomic clones carrying the wild-type *his-9(+)* or a mutant *his-9(Q125ochre)* gene and three wild-type histone genes (*his-10, his-11*, and *his-12*) located 5′ upstream of *his-9* (Figure 1F). Because our gene-dosage study indicated that *n5357* is a gain-of-function mutation, we introduced the *his-9(Q125ochre)* clone into wild-type animals. We observed that wild-type animals carrying the *his-9(Q125ochre)* clone displayed MI transformation (Figure 1F). By contrast, the MI neuron was not transformed in wild-type animals carrying the wild-type *his-9(+)* clone (Figure 1F). In addition, a frameshift mutation in the *his-9* locus of the *his-9(Q125ochre)* clone prevented transformation of MI (Figure 1F). These results further indicate that *n5357* is a gain-of-function allele of *his-9*.

Mutant H3 Lacking H3-H3 Interaction Sites Causes MI Transformation

During nucleosome assembly, a histone H3 protein binds to a histone H4 protein to form an H3-H4 dimer, and two H3-H4 dimers bind through an interaction between two H3 proteins to form an H3-H4 tetramer (Luger et al., 1997). Based on the crystal structure of the nucleosome core particle (Luger et al., 1997), we postulated that the *his-9(Q125ochre)* mutation eliminates two residues, leucine 126 and isoleucine 130, engaged in the H3-H3 interaction (Figure 2A). That the *his-9(n5357)* mutant phenotype is cold sensitive is consistent with the hypothesis that an abnormality in a protein-protein interaction causes the *his-9* gain-of-function activity (Richards et al., 2000). To test this hypothesis, we introduced into wild-type animals *his-9* genomic clones in which the *his-9* coding sequences were truncated at the glutamine 125 codon *(ΔQ125-A135),* the arginine 116 codon *(ΔR116-A135)*, or the aspartic acid 106 codon *(ΔD106-A135)* (Figure 2B). All of these mutant *his-9* clones eliminated HIS-9 residues important for the H3-H3 interaction, and all caused MI transformation (Figure 2B).

Based on nucleosome crystal structure, H3-H3 interaction is mediated in part by a hydrogen bond between histidine 113 of one histone H3 protein and aspartic acid 123 of the second H3 molecule (Luger et al., 1997). To further test whether a lack of histone H3-H3 interaction sites causes the gain-of-function activity of *his-9*, we generated mutant *his-9* genomic clones in which the histidine 113 codon or the aspartic acid 123 codon was altered to an aspartic acid codon (H113D) or a histidine codon (D123H), respectively (Figure 2B). Introduction of these mutant *his-9* clones into wild-type animals caused MI transformation (Figure 2B). These results demonstrate that mutant HIS-9 proteins unable to form an H3-H4 tetramer through interaction with another H3 protein display a gain-of-function activity and cause the loss of the MI-e3D bilateral asymmetry.

his-9(gf) Acts in the MI Mother Cell to Cause the Loss of the MI-e3D Asymmetry

We next examined whether the *his-9* gain-of-function activity affects the left-right asymmetric expression of CEH-36, NGN-1, and/or HLH-2. We integrated wild-type and mutant *his-9* transgenes into *C. elegans* chromosomes and found that an integrated *his-9(H113D)* transgene caused the most severe MI transformation defect (Table S1). Expression of CEH-36, NGN-1, and HLH-2 remained left-right asymmetric in animals carrying the *his-9(+)* or *his-9(H113D)* transgene (Figures 3A–3C), indicating that the *his-9* gain-of-function activity affects a process downstream of or in parallel to the left-right asymmetric expression of CEH-36, NGN-1, and HLH-2.

To identify when and where *his-9* gain-of-function activity acts to cause the loss of the MI-e3D asymmetry, we performed a genetic mosaic analysis (Figure 3D). We generated animals carrying an extrachromosomal array containing the *his-9(H113D)* transgene marked with cell-autonomous *gfp* reporters *sur-5::gfp* and *unc-119::gfp* (Nakano et al., 2010). Extrachromosomal arrays in *C. elegans* are mitotically unstable, resulting in clones of cells that have lost the array. We used Nomarski optics and epifluorescence to examine animals carrying the *his-9(H113D)* transgene and determined in each animal (1) the fate of ABaraappaaa, i.e., an MI-neuronal fate or an e3D-like epithelial fate, judged by the size and morphology of its nucleus and (2) the cell division at which the *his-9(H113D)* transgene was lost, judged by the GFP fluorescence of cells derived from the ABara cell lineage (Figure 3D). This analysis of GFP fluorescence

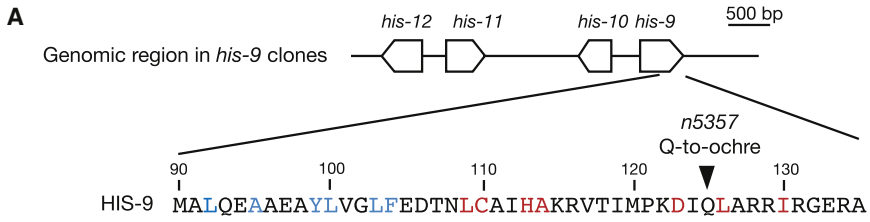

B

Genomic clone		% MI transformation 15 °C	% MI transformation 20 °C
his-9(+)	MALQEAAEAYLVGLFEDTNLCAIHAKRVTIMPKDIQLARRIRGERA	0 (*n* = 50)	0 (*n* = 118)
his-9(ΔQ125-A135)	MALQEAAEAYLVGLFEDTNLCAIHAKRVTIMPKDI	24 (*n* = 102)	28 (*n* = 122)
his-9(ΔR116-A135)	MALQEAAEAYLVGLFEDTNLCAIHAK	28 (*n* = 90)	15 (*n* = 84)
his-9(ΔD106-A135)	MALQEAAEAYLVGLFED	4 (*n* = 115)	25 (*n* = 109)
his-9(H113D)	MALQEAAEAYLVGLFEDTNLCAIDAKRVTIMPKDIQLARRIRGERA	22 (*n* = 73)	43 (*n* = 102)
his-9(D123H)	MALQEAAEAYLVGLFEDTNLCAIHAKRVTIMPKHIQLARRIRGERA	14 (*n* = 80)	3 (*n* = 108)

Figure 2. Mutations that Alter the C Terminus of HIS-9 Cause Loss of the MI-e3D Asymmetry

(A) Genomic region present in *his-9* clones, the amino acid sequence of a region of HIS-9, and the site of the *n5357* mutation are shown. Residues in blue and red are involved in interactions with histones H4 and H3, respectively.

(B) The predicted HIS-9 amino acid sequence of each genomic clone and percentages of animals with the MI transformation defect are shown. Residues substituted by mutagenesis are shown in green.

See also Table S1.

allowed us to determine the precise cell division at which an array loss occurred among the cell divisions of ABara descendants that give rise to the postmitotic ABaraappaaa. (We could not analyze the cell division of the MI mother cell ABaraappaa because the MI sister cell becomes the m1DR pharyngeal muscle cell, and m1DR fuses with five other m1 muscle cells later in development [Albertson and Thomson, 1976]. Thus, GFP fluorescence in m1DR might not represent the inheritance of the array to m1DR but rather result from the presence of the array in any of the five other m1 muscle cells derived from other cell lineages.) In our experiment, animals in which the array was lost at the division of the MI mother cell would have been counted as animals in which the array loss occurred at the previous cell division, that of ABaraappa, the MI grandmother cell.

We observed that none of the 45 animals in which the array loss had occurred at or prior to the division of ABaraapp showed MI transformation (Figure 3D). By contrast, of 686 animals in which the *his-9(H113D)* array was present in the postmitotic ABaraappaaa cell, 293 animals (43%) displayed MI transformation (Figure 3D), suggesting that *his-9* gain-of-function activity acts cell-autonomously to cause MI transformation. In addition, we identified 38 animals in which the array had been lost at the cell division of either ABaraappa or ABaraappaa. Three of these thirty-eight animals (3%) showed MI transformation (Figure 3D). This low fraction of MI transformation compared to that of the animals in which the array was present in the postmitotic ABaraappaaa cell (43%) likely reflects two groups among the 38 animals, one in which the array had been lost at the ABaraappa division and another in which the array loss had occurred at the ABaraappaa division. Together these observations suggest that the presence of the *his-9(H113D)* transgene in ABaraappaa, the MI mother cell, is sufficient to cause MI transformation. We concluded that *his-9* gain-of-function activity cell-autonomously acts in the MI mother cell to cause MI transformation.

The MI Fate Specification Is Sensitive to Histone H3 Mutations

his-9(n5357) animals are grossly normal, and we did not identify defects in the generation of other pharyngeal cells in these mutant animals. Given this specific effect of *his-9* gain-of-function activity, we asked whether expression of *his-9* is restricted to the cell lineage that gives rise to MI. We generated wild-type *his-9(+)* and mutant *his-9(H113D)* translational *mStrawberry* fusion transgenes and found that *his-9(H113D)::mStrawberry* but not *his-9(+)::mStrawberry* caused MI transformation (Figure 4A), suggesting that these *his-9* trangenes are functional. Both *his-9(+)::mStrawberry* and *his-9(H113D)::mStrawberry* localized to nuclei of many cells, including MI, e3D, and the extra e3D-like cell (Figure 4A), indicating that *his-9* is broadly expressed.

Given the presence in the *C. elegans* genome of 13 additional replication-dependent histone H3 genes that encode proteins with amino acid sequences identical to that of HIS-9 (Figure 4B), we asked whether mutations in these histone H3 genes could

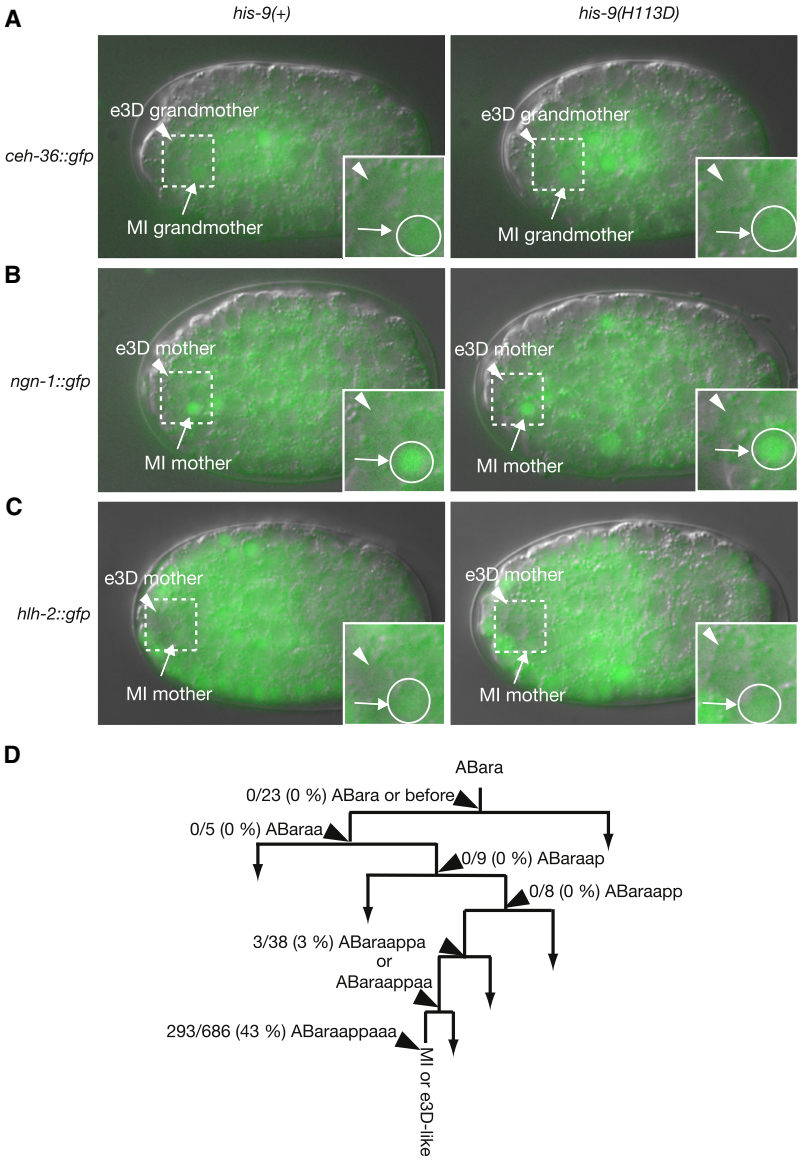

Figure 3. *his-9(gf)* Acts in the MI Mother Cell

(A–C) Embryos carrying *his-9(+)* (the left column) or *his-9(H113D)* (the right column) transgenes with *ceh-36::gfp* (A), *ngn-1::gfp* (B), or *hlh-2::gfp* (C) reporters. Insets show magnified views of the boxed regions. Arrows indicate the MI grandmother cell and the MI mother cell. Arrowheads indicate the e3D grandmother cell and the e3D mother cell. White circles indicate the positions of the MI grandmother cell (A) and the MI mother cell (B and C). GFP expression was observed in the MI progenitor cells but not in the e3D progenitor cells.

(D) Mosaic analysis of *his-9(gf).* A portion of the cell lineage showing the origin of ABaraappaaa is shown. The numbers represent the fractions of the animals with the MI transformation defect in which the *his-9(H113D)* extrachromosomal array was lost at the corresponding cell division. The experiment was performed and analyzed as described (Nakano et al., 2010).

also cause MI transformation. We generated wild-type (+) and mutant *(H113D)* transgenes of three additional histone H3 genes, *his-2(V), his-13(II)*, and *his-32(IV),* and found that none of the wild-type transgenes caused MI transformation (Figure 4B). By contrast, all three of the mutant histone H3 transgenes caused MI transformation but no other gross abnormalities (Figure 4B). These observations suggest that MI cell-fate specification involves a mechanism that is markedly sensitive to gain-of-function mutations in histone H3 genes.

CAF-1 Is Required for the MI-e3D Asymmetry

The human CAF-1 protein complex deposits histones H3-H4 into nucleosomes for DNA-replication-dependent nucleosome assembly (Smith and Stillman, 1989). CAF-1 is composed of three subunits, p150, p60, and p48 (Kaufman et al., 1995; Verreault et al., 1996), and preferentially binds to a histone H3-H4 complex that contains the replication-dependent histone H3.1 (Tagami et al., 2004). The *C. elegans* genome encodes proteins homologous to the CAF-1 subunits, including the p150 homolog T06D10.2, the p60 homolog Y71G12B.1, and the p48 homologs LIN-53 (Lu and Horvitz, 1998) and RBA-1 (Solari and Ahringer, 2000). We named *T06D10.2* and *Y71G12B.1 chaf-1* and *chaf-2* (*ch*romatin *a*ssembly *f*actor), respectively. Inactivation of *chaf-1, chaf-2*, or *rba-1* but not *lin-53* by RNA interference (RNAi) caused MI transformation (Figure 5 and unpublished data); in addition, RNAi treatment of any of these four genes caused incompletely penetrant embryonic lethality (data not shown). We also isolated deletion alleles of *chaf-1* and *rba-1* (Figure S2). Both deletion mutants displayed maternal-effect embryonic lethality, but *chaf-1(n5453Δ)* and *rba-1(n5418Δ)* deletion homozygous animals derived from their respective heterozygous mothers did not show MI transformation (Table S2). Given that RNAi of *chaf-1* and *rba-1* caused MI transformation, these observations suggest that the MI transformation defect of *chaf-1* and *rba-1* mutants might be maternally rescued. We therefore tested whether the zygotic loss of *chaf-1* and *rba-1* activity sensitizes *his-9(gf)* mutants to the MI transformation defect. Indeed, we observed that *chaf-1(n5453Δ)* and *rba-1(n5418Δ)* each enhanced the MI transformation defect of *his-9(n5357)* animals (Table S2). We conclude that the *C. elegans* CAF-1 complex is required to establish the MI-e3D asymmetry.

Human CAF-1 has been shown to interact with the proliferating cell nuclear antigen PCNA (Shibahara and Stillman, 1999). PCNA associates with replicated DNA and helps mark newly replicated DNA for CAF-1-mediated chromatin assembly. We therefore asked whether the *C. elegans* ortholog of PCNA, *pcn-1,* is required to establish the MI-e3D asymmetry. We observed that RNAi treatment of *pcn-1* caused MI

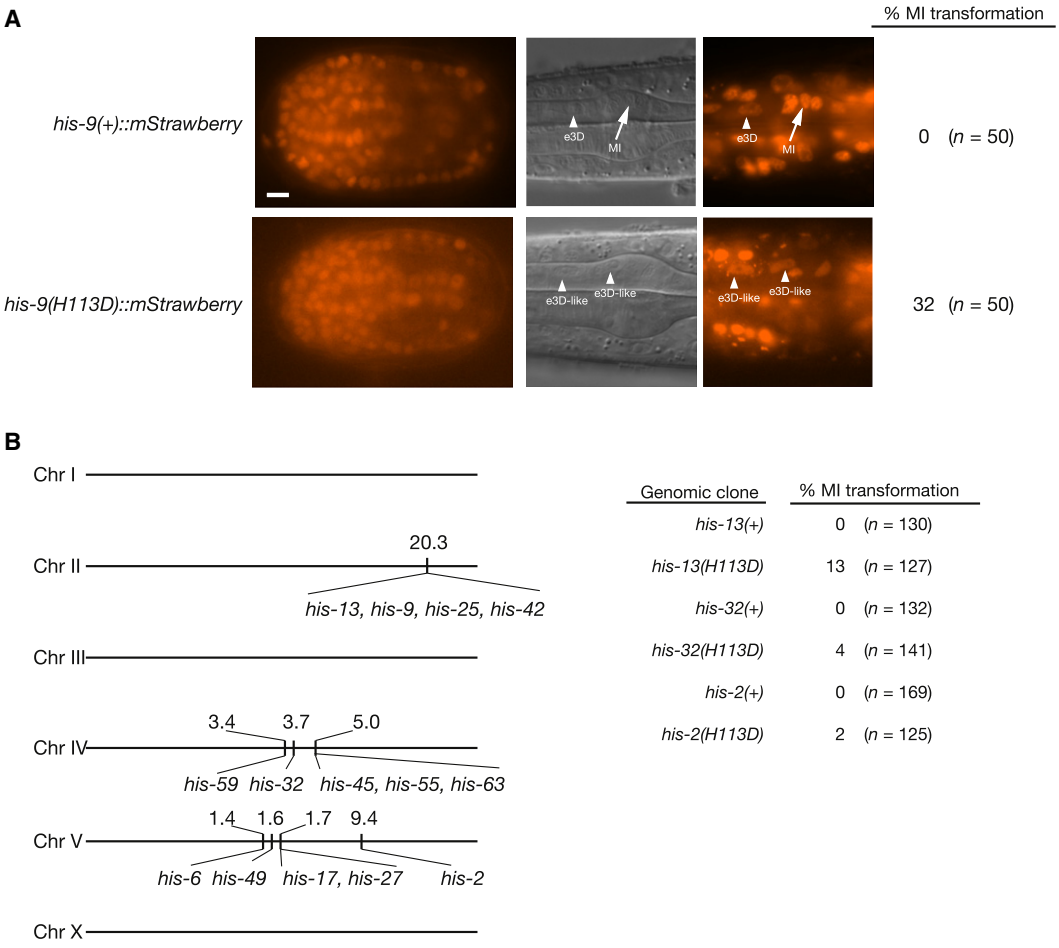

Figure 4. MI Fate Specification Is Sensitive to Histone H3 Mutations

(A) Expression of translational *his-9(+)::mStrawberry* (top panel) and *his-9(H113D)::mStrawberry* (bottom panel) genes during embryonic (left panel) and larval (right panel) stages. Nomarski images (middle panel) of the same larvae and percentages of animals with the MI transformation defect are shown. Arrows indicate the MI neuron, and arrowheads indicate the e3D and the e3D-like epithelial cells. Scale bar, 5 μm.

(B) The genomic positions of *his-9* and 13 additional replication-dependent histone H3 genes that encode proteins with amino acid sequences identical to that of HIS-9 are shown. Numbers represent approximate genetic map positions. Percentages of animals with the MI transformation defect are shown.

transformation (Figure 5). Thus, *pcn-1* is also required to generate the MI-e3D asymmetry. We suggest that replication-dependent nucleosome formation mediated by CAF-1 and PCN-1 is necessary to generate the MI-e3D asymmetry.

Drosophila dASF1 was identified as a factor that stimulates CAF-1-mediated nucleosome formation (Tyler et al., 1999). ASF1 was shown to bind to an H3-H4 dimer (English et al., 2006; Natsume et al., 2007) and proposed to transfer an H3-H4 dimer to the CAF-1 complex (Loyola and Almouzni, 2004). We tested whether two *C. elegans* ASF1 homologs, *unc-85* and *asfl-1* (Grigsby and Finger, 2008), are required for the MI-e3D asymmetry. We observed that MI and e3D were correctly specified in *unc-85(ok2125Δ)* and *asfl-1(ok2060Δ)* mutants (Figure S2 and Table S3). *asfl-1(ok2060Δ); unc-85(ok2125Δ)* double mutants displayed sterility but did not show MI transformation (Table S3). We performed RNAi treatment of *asfl-1* and observed that *asf-1(RNAi); unc-85(ok2125Δ)* animals displayed incompletely penetrant embryonic lethality but did not exhibit MI transformation (Table S3). These results indicate that the establishment of the MI-e3D asymmetry does not require the two *C. elegans* homologs of ASF1, and that CAF-1 functions independently of the ASF1 proteins to establish the MI-e3D asymmetry.

Mutant HIS-9 Proteins Inhibit Nucleosome Assembly

That a defect in any of the three CAF-1 subunits caused precisely the same highly specific abnormality as the *his-9(n5357)* mutation strongly suggests that CAF-1-mediated nucleosome formation is impaired by mutant HIS-9 proteins. To test this hypothesis, we performed replication-coupled chromatin assembly reactions with wild-type and mutant histone H3 proteins (Smith and Stillman, 1989). We performed the in vitro replication of DNA plasmids carrying the SV40 origin in the presence of SV40 T antigen, a human cell cytosolic extract that contains both replication proteins and histones, and [α-^{32}P]dATP to label replicated DNA. The products of the

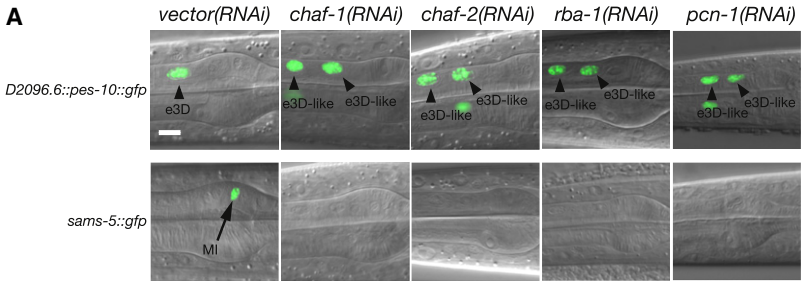

Figure 5. The CAF-1 Complex and PCN-1 Are Required to Establish the MI-e3D Bilateral Asymmetry

(A) Expression of *D2096.6::pes-10::gfp* e3D and *sams-5::gfp* MI reporters in progeny of animals grown on bacteria expressing double-strand RNA corresponding to control (vector) sequences or to genes encoding each member of the CAF-1 complex or to the *pcn-1* gene. Arrowheads indicate e3D and the extra e3D-like cell, and the arrow indicates MI. Scale bar, 5 μm.

(B) Percentage of animals showing the MI transformation defect.

See also Figure S2 and Tables S2 and S3.

B

RNAi treatment	% MI transformation	
vector	0	(*n* = 50)
chaf-1(RNAi)	32	(*n* = 125)
chaf-2(RNAi)	29	(*n* = 100)
rba-1(RNAi)	23	(*n* = 100)
pcn-1(RNAi)	17	(*n* = 172)

reactions were resolved by agarose electrophoresis and analyzed by autoradiography. As previously reported (Shibahara and Stillman, 1999; Smith and Stillman, 1989), in the absence of CAF-1, the products of the replication reaction were predominantly relaxed monomer circles (form I^0), as well as some topological isomers that migrated faster than form I^0 (Figure 6A). The addition of purified human CAF-1 promoted nucleosome assembly and changed the distribution of the labeled DNA from relaxed circular DNA to supercoiled DNA (Figure 6A; form I). Addition of purified histone H3-H4 complex carrying mutant histone H3(H113D) protein drastically reduced the level of supercoiled DNA (Figures 6A and 6B). We also observed that addition of H3(ΔQ125-A135)-H4 protein caused a reduction in the level of supercoiled DNA, albeit to a lesser degree than did H3(H113D)-H4 complex (Figures 6A and 6B). These observations are consistent with the magnitudes of the in vivo effects caused by the corresponding *his-9* mutations, as *his-9(H113D)* caused a stronger MI transformation defect than did *his-9(ΔQ125-A135)* (Figure 2 and Table S1). By contrast, addition of the wild-type H3-H4 complex did not reduce the fraction of supercoiled DNA. These results demonstrate that the mutant histone H3 proteins inhibit CAF-1-mediated nucleosome formation.

DISCUSSION

We report the isolation of the first mutant histone allele recovered from a genetic screen of a multicellular organism. This mutation, a gain-of-function allele of the *C. elegans* histone H3 gene *his-9,* causes an unexpectedly specific defect: the establishment of the MI-e3D bilateral asymmetry is disrupted. The *his-9* gain-of-function activity acts cell-autonomously in the MI mother cell and affects a process downstream of or parallel to the left-right asymmetric expression of the transcription factors NGN-1 and HLH-2. The CAF-1 protein complex is required for the MI-e3D asymmetry, and the mutant HIS-9 protein acts by inhibiting CAF-1-mediated nucleosome formation. These results suggest that CAF-1-mediated nucleosome assembly during S phase of the MI mother cell is required to specify the MI-neuronal fate. The newly assembled nucleosomes might then be transmitted to the postmitotic MI neuron and establish an MI-neuronal chromatin state.

It has been a matter of debate whether CAF-1, which interacts with histone H3.1 in mammalian cells (Tagami et al., 2004), binds to an H3-H4 dimer consisting of one H3 and one H4 polypeptide or an H3-H4 tetramer consisting of two H3 and two H4 polypeptides; it has also been unclear whether CAF-1 deposits an H3-H4 dimer or an H3-H4 tetramer onto replicating DNA (Margueron and Reinberg, 2010; Ransom et al., 2010; Tagami et al., 2004; Xu et al., 2010). These issues are important for understanding the mechanistic basis of epigenetic inheritance of histone modifications: if CAF-1 binds to and deposits a single H3-H4 dimer, parental H3-H4 tetramers might be split and distributed onto daughter DNA strands as two H3-H4 dimers, each of which could then be paired with a newly synthesized H3-H4 dimer, thereby propagating parental histone modifications to the two daughter DNA strands (Tagami et al., 2004); by contrast, a parental H3-H4 tetramer would be segregated to only one of the two daughter DNA strands if CAF-1 binds to and deposits an H3-H4 tetramer or if two CAF-1 proteins each bind to an H3-H4 dimer and interact and then together deposit an H3-H4 tetramer (Jackson, 1988; Leffak et al., 1977; Xu et al., 2010). Our results demonstrate that mutant HIS-9 proteins inhibit CAF-1-mediated nucleosome formation even in the presence of wild-type H3 proteins. This observation suggests that mutant HIS-9 proteins have a dominant-negative effect and act to reduce the level of functional CAF-1 by directly interacting with CAF-1. Because mutant HIS-9 proteins are likely defective in H3-H4 tetramer formation and hence able to form a HIS-9-H4 dimer but not an H3-H4 tetramer, our findings strongly support the model that CAF-1 binds to an H3-H4 dimer. Given a previous report that CAF-1-CAF-1 dimer interaction is important for chromatin assembly (Quivy et al., 2001), we suggest that the mutant HIS-9 H3.1-like protein forms a dimer with a histone H4 protein, and then this mutant HIS-9-H4 dimer binds to CAF-1, forming a complex unable to interact with a second CAF-1-H3-H4 complex through the H3-H3 interaction surface and a CAF-1-CAF-1 dimer interaction surface; in this way, the mutant HIS-9 protein could reduce the level of functional CAF-1 (Figure 6C).

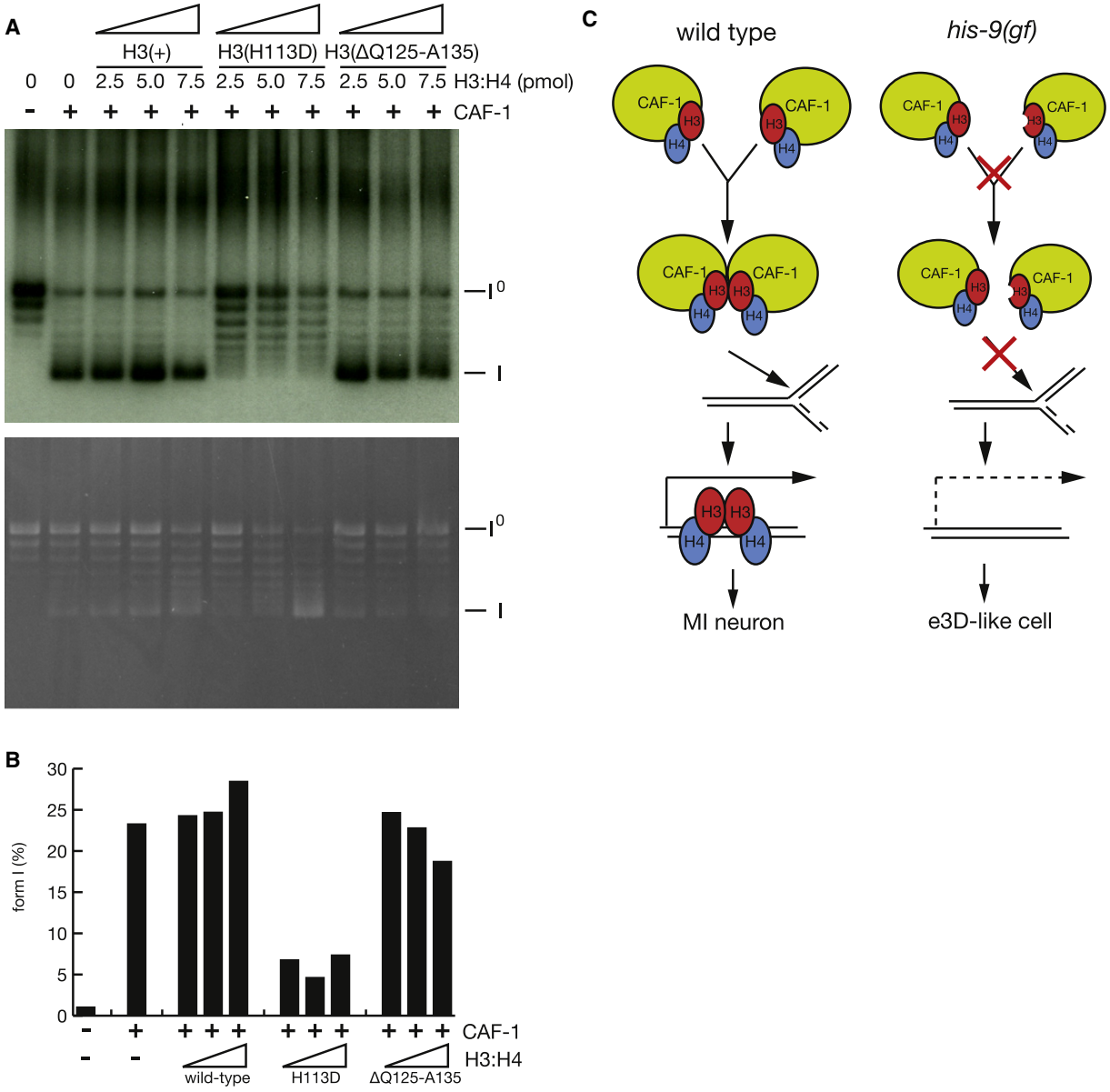

Figure 6. Mutant H3 Histone Proteins Inhibit CAF-1-Mediated Nucleosome Assembly

(A) Newly replicated DNA as visualized by autoradiography (upper panel) and total DNA visualized by staining with ethidium bromide (lower panel) are shown. The degree of nucleosome assembly was determined by the superhelical state of radiolabeled DNA. Migration of relaxed circular DNA (form I^0) and negatively supercoiled DNA (form I) are indicated. The presence or absence of CAF-1 and the amount of wild-type or mutant histone H3 complex with wild-type H4 in each reaction are shown.

(B) Quantification of the percentage of form I in the newly replicated monomer DNA in each reaction shown in (A).

(C) A Model for inhibition of CAF-1-mediated nucleosome assembly by mutant HIS-9 proteins. In the wild-type, each CAF-1 complex binds to a histone H3-H4 dimer. Two CAF-1-H3-H4 complexes are tethered through interactions between the two H3 molecules and between the two CAF-1 molecules prior to the deposition of the histone H3-H4 tetramer onto a locus required to promote the generation of the MI neuron. In *his-9(gf)* mutants, a mutant HIS-9 protein binds to a histone H4 protein to form a mutant HIS-9-H4 dimer. CAF-1 bound by a mutant HIS-9-H4 dimer cannot interact with a second CAF-1 complex containing a wild-type H3-H4 dimer and hence cannot complete nucleosome assembly.

Thus, our results suggest that during normal replication-coupled chromatin assembly, CAF-1 binds to an H3-H4 dimer, and that two CAF-1-H3-H4 complexes assemble to form an H3-H4 tetramer, thereby depositing an H3-H4 tetramer that consists entirely of newly synthesized H3 and H4 proteins. During this process of DNA replication, a parental H3-H4 tetramer remains intact and is transferred to newly replicated DNA.

Our observations also reveal that the two *C. elegans* homologs of ASF1 are not required to establish the MI-e3D asymmetry, indicating that an ASF1-independent pathway exists that

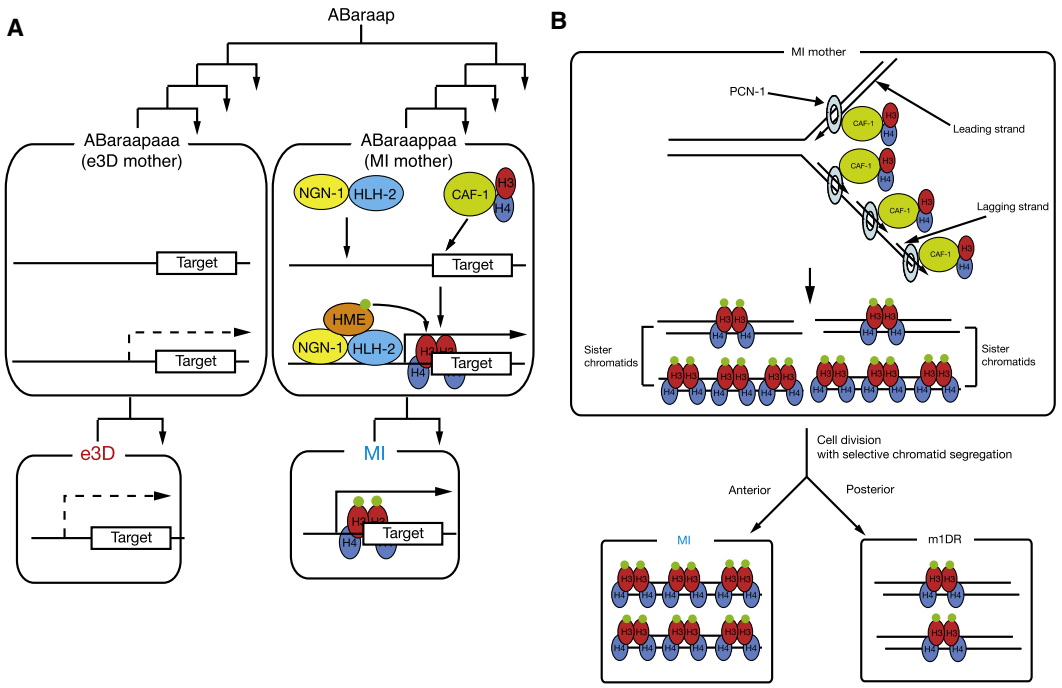

Figure 7. Model for the Specification of MI by the CAF-1-PCN-1 Complex

(A) CAF-1 assembles nucleosomes at NGN-1/HLH-2 target loci during S phase of the MI mother cell. The NGN-1/HLH-2 complex recruits a histone-modifying enzyme (HME) that generates epigenetic marks on the newly assembled nucleosomes. The newly assembled and epigenetically marked nucleosomes are transmitted to the postmitotic MI neuron, leading to the specification of the MI neuron. Green circles represent a posttranslational modification. (See text for details.)

(B) During DNA replication in the MI mother cell, PCN-1 promotes continuous DNA synthesis on the leading strands, and one PCN-1 clamp is required per initiation event; for the lagging-strand synthesis, one PCN-1 is required every Okazaki fragment, about 100–200 bp (Burhans et al., 1990). Differing amounts of PCN-1 associated with the two strands recruit differing amounts of CAF-1 and lead to differences in the densities of newly assembled nucleosomes at loci required to specify the MI fate between the two sister chromatids. Selective segregation of these epigenetically distinct chromatids marked with differing nucleosomal density results in the specification of the MI neuron.

leads to complex formation between CAF-1 and an H3-H4 dimer.

We previously showed that the specification of the MI-e3D asymmetry occurs at least three cell generations prior to the generation of MI and e3D within two sister cells, ABaraapa and ABaraapp, that first separate the left and right branches of the ABaraap cell lineage (Nakano et al., 2010). This initial asymmetry is transduced into the MI mother cell by a CEH-36/NGN-1/HLH-2 transcriptional cascade that acts through multiple rounds of cell divisions. The CEH-36 protein is present in the MI grandmother cell and promotes expression of two proneural bHLH proteins, NGN-1 and HLH-2. The NGN-1 and HLH-2 proteins form a dimer and are present in the MI mother cell. Given previous reports that mammalian homologs of these bHLH proteins regulate histone modifications (Beck et al., 2009; Pujadas et al., 2011), we suggest that the NGN-1/HLH-2 complex recruits histone-modifying enzymes that act on the nucleosomal arrays assembled by CAF-1 to generate epigenetic marks necessary for the specification of the MI neuron (Figure 7A). The molecular memory of the developmental cue established by the CEH-36/NGN-1/HLH-2 pathway might be transmitted to the postmitotic MI neuron by CAF-1-mediated replication-coupled chromatin assembly in the MI mother cell, generating a stable mark of the MI-neuronal chromatin state. In addition, because expression of NGN-1 and HLH-2 is left-right asymmetric and these proteins are present in the MI mother cell but not in the e3D mother cell (Nakano et al., 2010), CAF-1 and the NGN-1/HLH-2 complex likely establish a left-right asymmetry in chromatin states to generate the MI-e3D asymmetry.

The effect of the gain-of-function mutations in histone H3 genes is strikingly specific to MI cell-fate specification, which suggests that a mechanism of specifying the MI neuron is particularly sensitive to histone H3 gain-of-function mutations. One possible mechanism could be the generation of differing nucleosome densities at a locus important for MI cell-fate specification between two sister chromatids during S phase of the MI mother cell (Figure 7B). Specifically, it has been proposed that human CAF-1 and PCNA can generate a difference in the densities of newly synthesized nucleosomes at a given locus between two sister chromatids (Shibahara and Stillman, 1999). Upon selective segregation of chromatids, such distinct chromatin complexes would generate a difference between sister cells during development. MI fate specification could involve such a mechanism, so that during S phase of the MI mother cell, PCN-1 and CAF-1 generate differing nucleosome densities between two sister chromatids at loci required to specify the MI-neuronal fate. We

propose that such newly synthesized nucleosomes are modified by the NGN-1/HLH-2 complex, leading to the generation of differing densities of modified histones between two sister chromatids. There would then be a selective inheritance of these distinct chromatin structures to the MI neuron and its sister m1DR muscle cell (Figure 7B). In this way, both NGN-1/HLH-2-mediated histone modifications and CAF-1-mediated specific nucleosome density would be required for expression of target genes necessary to specify the MI-neuronal fate.

An alternative possibility is that the NGN-1/HLH-2 complex and CAF-1 could act on distinct sets of target genes. In this case, the NGN-1/HLH-2 complex might modify histones at one locus that are deposited by a replication-independent pathway, and CAF-1/PCN-1 might generate differing nucleosome densities at another locus between sister chromatids. Nonetheless, the simplest hypothesis is that both act on the same target genes to together control distinct aspects of a left-right asymmetric epigenetic regulation that specifies the MI bilateral asymmetry.

Such a mechanism of selective inheritance of sister chromatids might also be involved in left-right axis determination in mammals. *inversus viscerum* (*iv*) mutant mice were originally reported to show randomized directionality of their visceral asymmetries (Hummel and Chapman, 1959). The *iv* locus encodes a microtubule-based motor protein, called left-right dynein (LRD) (Supp et al., 1997), that is required for nodal cilia motility and nodal flow (Okada et al., 1999). Interestingly, LRD has been implicated in the biased chromatid segregation of mouse chromosome 7 in embryonic stem cells, endoderm, and neuroectoderm (Armakolas and Klar, 2007), and recently it was reported that the *iv* mutant hippocampus exhibits a loss of bilateral asymmetry rather than randomized directionality of the asymmetry (Kawakami et al., 2008). Our findings provide a link between these observations and suggest that LRD might promote a nervous system bilateral asymmetry through biased segregation of chromatids in a manner independent of nodal signaling. We suggest that selective segregation of chromatids marked with distinct chromatin states could be a conserved epigenetic mechanism that generates bilateral asymmetries in the nervous system in organisms as distant as nematodes and mammals.

EXPERIMENTAL PROCEDURES

C. elegans Strains

C. elegans strains were grown as described (Brenner, 1974). N2 (Bristol) was the wild-type strain. All strains were cultured at 20°C unless otherwise indicated. Germline transformation experiments were performed as described (Mello et al., 1991). A description of the plasmid constructs and concentrations used is available from the authors. The following extrachromosomal arrays, integrants, duplication chromosomes, and mutations were used and have been described (Riddle et al., 1997), except those from this study or otherwise indicated:

LG*I*: *rba-1(n5418Δ)* (this study), *chaf-1(n5453Δ)* (this study), *asfl-1(ok2060Δ)* (*ok2060Δ* was provided by the *C. elegans* Gene Knockout Consortium).

LG*II*: *unc-85(ok2125Δ)* (*ok2125Δ* was provided by the *C. elegans* Gene Knockout Consortium), *rol-1(e91), his-9(n5357)* (this study), *unc-52(e444), nIs447[his-9(+), unc-76(+), tph-1::mStrawberry]* (this study).

LG*III*: *nIs394[ngn-1::gfp, lin-15AB(+)]* (Nakano et al., 2010).

LG*IV*: *unc-76(e911), nIs407[hlh-2::gfp, lin-15AB(+)]* (Nakano et al., 2010), *nIs451[his-9(H113D), unc-76(+), unc-25::mStrawberry]* (this study).

LG*V*: *nIs396[sams-5::gfp, lin-15AB(+)]* (Nakano et al., 2010).

LG*X*: *nIs445[ceh-36::gfp, lin-15AB(+)]* (Nakano et al., 2010), *nIs363 [D2096.6::pes-10::gfp, lin-15AB(+)]* (Nakano et al., 2010), *nIs448[his-9(Q125ochre), unc-76(+), tph-1::mStrawaberry], nIs449[his-9(ΔQ125-A135), unc-76(+), tph-1::mStrawberry], nIs452[his-9(D123H), unc-76(+), sre-1::mStrawberry]* (all this study).

Free duplications and extrachromosomal arrays: *mnDp34(II;f)* (Edgley et al., 2006), *nEx1708[his-9(+), unc-76(+), tph-1::mStrawberry], nEx1709[his-9(Q125ochre), unc-76(+), tph-1::mStrawberry], nEx1711[his-9(H113D), unc-76(+), unc-25::mStrawberry], nEx1712[his-9(D123H), unc-76(+), sre-1::mStrawberry], nEx1713[his-9(f.s. Q125ochre), unc-76(+), tph-1::mStrawberry], nEx1714[his-9(ΔQ125-A135), unc-76(+), tph-1::mStrawberry], nEx1720[his-9(H113D), unc-76(+), unc-119::gfp, sur-5::gfp], nEx1723[his-9(ΔR116-A135), unc-76(+), tph-1::mStrawberry], nEx1724[his-9(ΔD106-A135), unc-76(+), tph-1::mStrawberry], nEx1736[his-32(H113D), unc-76(+)], nEx1737[his-2(H113D), unc-76(+)], nEx1738[his-32(+), unc-76(+)], nEx1739[his-2(+), unc-76(+)], nEx1740[his-13(+), unc-76(+)], nEx1741[his-13(H113D), unc-76(+)], nEx1742[his-9(+)::mStrawberry, unc-76(+)], nEx1743[his-9(H113D)::mStrawberry, unc-76(+)]* (all this study).

Isolation of *his-9(n5357), chaf-1(n5453Δ)*, and *rba-1(n5418Δ)*

We mutagenized wild-type animals carrying the *D2096.6::pes-10::gfp* reporter with ethyl methanesulfonate (EMS), and F_3 progeny were observed using a fluorescence-equipped dissecting microscope. *his-9(n5357)* was isolated in an animal that contained an extra cell expressing the *D2096.6::pes-10::gfp* reporter. To isolate deletion alleles of *chaf-1* and *rba-1,* we screened by PCR genomic DNA pools from EMS-mutagenized animals for deletion alleles of *chaf-1* and *rba-1*, essentially as described (Liu et al., 1999). The *chaf-1(n5453Δ)* and *rba-1(n5418Δ)* alleles removed sequences between nucleotides 9937 and 10864 of cosmid T06D10 and between nucleotides 35977 and 37677 of cosmid K07A1, respectively.

Gene-Dosage Study of *n5357*

We allowed hermaphrodites of genotype *rol-1(e91) n5357 unc-52(e444); nIs363; mnDp34* to self-fertilize at 15°C and determined the MI transformation defect of their Rol Unc and non-Rol non-Unc progeny at 15°C. We noted that the MI transformation defect of animals of genotype *rol-1 n5357 unc-52/rol-1 n5357 unc-52* shown in Figure 1D was less severe than that of animals of genotype *n5357/n5357* shown in Figure 1C. We found that this difference in the penetrance of the MI transformation defects was caused by the presence of a mutation(s) that partially suppresses MI transformation and is derived from strains carrying *unc-52(e444)*. The existence of this mutation, which was present in the two strains used in Figure 1D but was absent in all other strains used in this work, does not affect any of our conclusions. We did not further study this suppressor activity.

Mapping of *n5357*

We crossed *rol-1(e91) n5357 unc-52(e444)* animals with the wild-type polymorphic strain CB4856 and isolated F_2 Rol non-Unc progeny, determined the presence or absence of *n5357*, and identified crossover sites, essentially as described (Wicks et al., 2001). We mapped *n5357* to a 55 kb interval between nucleotides 13781415 and 13837046 of LG*II*.

Supercoiling Assay

Wild-type and mutant histone proteins were purified as described (Luger et al., 1999).

The supercoiling assay was performed as described (Smith and Stillman, 1989) with minor modifications: each reaction (25 μl) contained 50 fmol of plasmid pSV011 with or without 37.5 fmol of purified CAF-1 proteins. Reactions were incubated at 37°C for 60 min.

SUPPLEMENTAL INFORMATION

Supplemental Information includes two figures and three tables and can be found with this article online at doi:10.1016/j.cell.2011.11.053.

ACKNOWLEDGMENTS

We thank P. Wendel for her help with the supercoiling assay; A. Fire for expression vectors; the *Caenorhabditis* Genetics Center, which is funded by the NIH National Center for Research Resources (NCRR), for strains; N. An, R. Droste, and T. Ljungars for technical assistance; and D. Denning, K. Boulias, and M. Nakano for comments about the manuscript. H.R.H. is an Investigator of the Howard Hughes Medical Institute and the David H. Koch Professor of Biology at MIT. This work was supported by the Howard Hughes Medical Institute and a grant from the National Cancer Institute (CA13106).

Received: July 5, 2011
Revised: September 26, 2011
Accepted: November 29, 2011
Published online: December 15, 2011

REFERENCES

Albertson, D.G., and Thomson, J.N. (1976). The pharynx of *Caenorhabditis elegans*. Philos. Trans. R. Soc. Lond. B Biol. Sci. *275*, 299–325.

Armakolas, A., and Klar, A.J. (2007). Left-right dynein motor implicated in selective chromatid segregation in mouse cells. Science *315*, 100–101.

Beck, K., Peak, M.M., Ota, T., Nemazee, D., and Murre, C. (2009). Distinct roles for E12 and E47 in B cell specification and the sequential rearrangement of immunoglobulin light chain loci. J. Exp. Med. *206*, 2271–2284.

Brenner, S. (1974). The genetics of *Caenorhabditis elegans*. Genetics *77*, 71–94.

Burhans, W.C., Vassilev, L.T., Caddle, M.S., Heintz, N.H., and DePamphilis, M.L. (1990). Identification of an origin of bidirectional DNA replication in mammalian chromosomes. Cell *62*, 955–965.

Edgley, M.L., Baillie, D.L., Riddle, D.L., and Rose, A.M. (2006). Genetic balancers. WormBook. Published online April 6, 2006. 10.1895/wormbook.1.89.1. http://www.wormbook.org.

English, C.M., Adkins, M.W., Carson, J.J., Churchill, M.E., and Tyler, J.K. (2006). Structural basis for the histone chaperone activity of Asf1. Cell *127*, 495–508.

Escalante-Mead, P.R., Minshew, N.J., and Sweeney, J.A. (2003). Abnormal brain lateralization in high-functioning autism. J. Autism Dev. Disord. *33*, 539–543.

Grigsby, I.F., and Finger, F.P. (2008). UNC-85, a *C. elegans* homolog of the histone chaperone Asf1, functions in post-embryonic neuroblast replication. Dev. Biol. *319*, 100–109.

Hamada, H. (2008). Breakthroughs and future challenges in left-right patterning. Dev. Growth Differ. *50* (*Suppl 1*), S71–S78.

Hobert, O., Johnston, R.J., Jr., and Chang, S. (2002). Left-right asymmetry in the nervous system: the *Caenorhabditis elegans* model. Nat. Rev. Neurosci. *3*, 629–640.

Hummel, K.P., and Chapman, D.B. (1959). Visceral inversion and associated anomalies in the mouse. J. Hered. *50*, 9–13.

Jackson, V. (1988). Deposition of newly synthesized histones: hybrid nucleosomes are not tandemly arranged on daughter DNA strands. Biochemistry *27*, 2109–2120.

Kaufman, P.D., Kobayashi, R., Kessler, N., and Stillman, B. (1995). The p150 and p60 subunits of chromatin assembly factor I: a molecular link between newly synthesized histones and DNA replication. Cell *81*, 1105–1114.

Kawakami, R., Shinohara, Y., Kato, Y., Sugiyama, H., Shigemoto, R., and Ito, I. (2003). Asymmetrical allocation of NMDA receptor ε2 subunits in hippocampal circuitry. Science *300*, 990–994.

Kawakami, R., Dobi, A., Shigemoto, R., and Ito, I. (2008). Right isomerism of the brain in inversus viscerum mutant mice. PLoS One *3*, e1945.

Leffak, I.M., Grainger, R., and Weintraub, H. (1977). Conservative assembly and segregation of nucleosomal histones. Cell *12*, 837–845.

Levin, M. (2005). Left-right asymmetry in embryonic development: a comprehensive review. Mech. Dev. *122*, 3–25.

Li, X., Branch, C.A., Ardekani, B.A., Bertisch, H., Hicks, C., and DeLisi, L.E. (2007). fMRI study of language activation in schizophrenia, schizoaffective disorder and in individuals genetically at high risk. Schizophr. Res. *96*, 14–24.

Liu, L.X., Spoerke, J.M., Mulligan, E.L., Chen, J., Reardon, B., Westlund, B., Sun, L., Abel, K., Armstrong, B., Hardiman, G., et al. (1999). High-throughput isolation of *Caenorhabditis elegans* deletion mutants. Genome Res. *9*, 859–867.

Loyola, A., and Almouzni, G. (2004). Histone chaperones, a supporting role in the limelight. Biochim. Biophys. Acta *1677*, 3–11.

Lu, X., and Horvitz, H.R. (1998). *lin-35* and *lin-53*, two genes that antagonize a *C. elegans* Ras pathway, encode proteins similar to Rb and its binding protein RbAp48. Cell *95*, 981–991.

Luger, K., Mäder, A.W., Richmond, R.K., Sargent, D.F., and Richmond, T.J. (1997). Crystal structure of the nucleosome core particle at 2.8 A resolution. Nature *389*, 251–260.

Luger, K., Rechsteiner, T.J., and Richmond, T.J. (1999). Preparation of nucleosome core particle from recombinant histones. Methods Enzymol. *304*, 3–19.

Margueron, R., and Reinberg, D. (2010). Chromatin structure and the inheritance of epigenetic information. Nat. Rev. Genet. *11*, 285–296.

Mello, C.C., Kramer, J.M., Stinchcomb, D., and Ambros, V. (1991). Efficient gene transfer in *C.elegans*: extrachromosomal maintenance and integration of transforming sequences. EMBO J. *10*, 3959–3970.

Nakano, S., Ellis, R.E., and Horvitz, H.R. (2010). Otx-dependent expression of proneural bHLH genes establishes a neuronal bilateral asymmetry in *C. elegans*. Development *137*, 4017–4027.

Natsume, R., Eitoku, M., Akai, Y., Sano, N., Horikoshi, M., and Senda, T. (2007). Structure and function of the histone chaperone CIA/ASF1 complexed with histones H3 and H4. Nature *446*, 338–341.

Okada, Y., Nonaka, S., Tanaka, Y., Saijoh, Y., Hamada, H., and Hirokawa, N. (1999). Abnormal nodal flow precedes situs inversus in *iv* and *inv* mice. Mol. Cell *4*, 459–468.

Pettitt, J., Crombie, C., Schümperli, D., and Müller, B. (2002). The *Caenorhabditis elegans* histone hairpin-binding protein is required for core histone gene expression and is essential for embryonic and postembryonic cell division. J. Cell Sci. *115*, 857–866.

Pujadas, G., Felipe, F., Ejarque, M., Sanchez, L., Cervantes, S., Lynn, F.C., Gomis, R., and Gasa, R. (2011). Sequence and epigenetic determinants in the regulation of the Math6 gene by Neurogenin3. Differentiation *82*, 66–76.

Quivy, J.P., Grandi, P., and Almouzni, G. (2001). Dimerization of the largest subunit of chromatin assembly factor 1: importance *in vitro* and during *Xenopus* early development. EMBO J. *20*, 2015–2027.

Ransom, M., Dennehey, B.K., and Tyler, J.K. (2010). Chaperoning histones during DNA replication and repair. Cell *140*, 183–195.

Richards, K.L., Anders, K.R., Nogales, E., Schwartz, K., Downing, K.H., and Botstein, D. (2000). Structure-function relationships in yeast tubulins. Mol. Biol. Cell *11*, 1887–1903.

Riddle, D.L., Blumenthal, T., Meyer, B.J., and Priess, J. (1997). *C. elegans* II (Plainview, NY: Cold Spring Harbor Laboratory Press).

Shibahara, K., and Stillman, B. (1999). Replication-dependent marking of DNA by PCNA facilitates CAF-1-coupled inheritance of chromatin. Cell *96*, 575–585.

Shiratori, H., and Hamada, H. (2006). The left-right axis in the mouse: from origin to morphology. Development *133*, 2095–2104.

Smith, S., and Stillman, B. (1989). Purification and characterization of CAF-I, a human cell factor required for chromatin assembly during DNA replication in vitro. Cell *58*, 15–25.

Solari, F., and Ahringer, J. (2000). NURD-complex genes antagonise Ras-induced vulval development in *Caenorhabditis elegans*. Curr. Biol. *10*, 223–226.

Sulston, J.E., Schierenberg, E., White, J.G., and Thomson, J.N. (1983). The embryonic cell lineage of the nematode *Caenorhabditis elegans*. Dev. Biol. *100*, 64–119.

Supp, D.M., Witte, D.P., Potter, S.S., and Brueckner, M. (1997). Mutation of an axonemal dynein affects left-right asymmetry in *inversus viscerum* mice. Nature *389*, 963–966.

Tagami, H., Ray-Gallet, D., Almouzni, G., and Nakatani, Y. (2004). Histone H3.1 and H3.3 complexes mediate nucleosome assembly pathways dependent or independent of DNA synthesis. Cell *116*, 51–61.

Toga, A.W., and Thompson, P.M. (2003). Mapping brain asymmetry. Nat. Rev. Neurosci. *4*, 37–48.

Tyler, J.K., Adams, C.R., Chen, S.R., Kobayashi, R., Kamakaka, R.T., and Kadonaga, J.T. (1999). The RCAF complex mediates chromatin assembly during DNA replication and repair. Nature *402*, 555–560.

Verreault, A., Kaufman, P.D., Kobayashi, R., and Stillman, B. (1996). Nucleosome assembly by a complex of CAF-1 and acetylated histones H3/H4. Cell *87*, 95–104.

Wicks, S.R., Yeh, R.T., Gish, W.R., Waterston, R.H., and Plasterk, R.H. (2001). Rapid gene mapping in *Caenorhabditis elegans* using a high density polymorphism map. Nat. Genet. *28*, 160–164.

Xu, M., Long, C., Chen, X., Huang, C., Chen, S., and Zhu, B. (2010). Partitioning of histone H3-H4 tetramers during DNA replication-dependent chromatin assembly. Science *328*, 94–98.